LoCuSS: Subaru Weak Lens Study of 30 Galaxy Clusters

Masahiro Takada

(IPMU, U. Tokyo)

IPMU INSTITUTE FOR THE PHYSICS AND MATHEMATICS OF THE UNIVERSE

@ Subaru/Gemini conference, Kyoto, May 19, 2009

Collaborators

Local Cluster Substructure Survey (LoCuSS)

T. Futamase (Tohoku U.)

N. Okabe

Y. Okura

K. Takahashi

K. Umetsu (ASIAA Taiwan)

M. Oguri (Stanford)

G. P. Smith (Birmingham)

+LoCuSS team members

This talk is mostly based on Okabe, MT et al. arXiv:0903.1103

Outline

- Introduction/Background
  - The importance of cluster mass estimation for cosmology
  - NFW profile: A test of CDM model
- What is LoCuSS?
- Results: weak lensing constraints for cluster mass distribution
  - Profile fitting
  - Aperture mass method
- Summary

- In a real world, there is no unique definition of cluster mass; no clear boundary with the surrounding structures
- Have to infer cluster masses (including DM) from the observables (optical, X-ray, *lensing*)
- Critically important to have the well-calibrated mass-observable relation

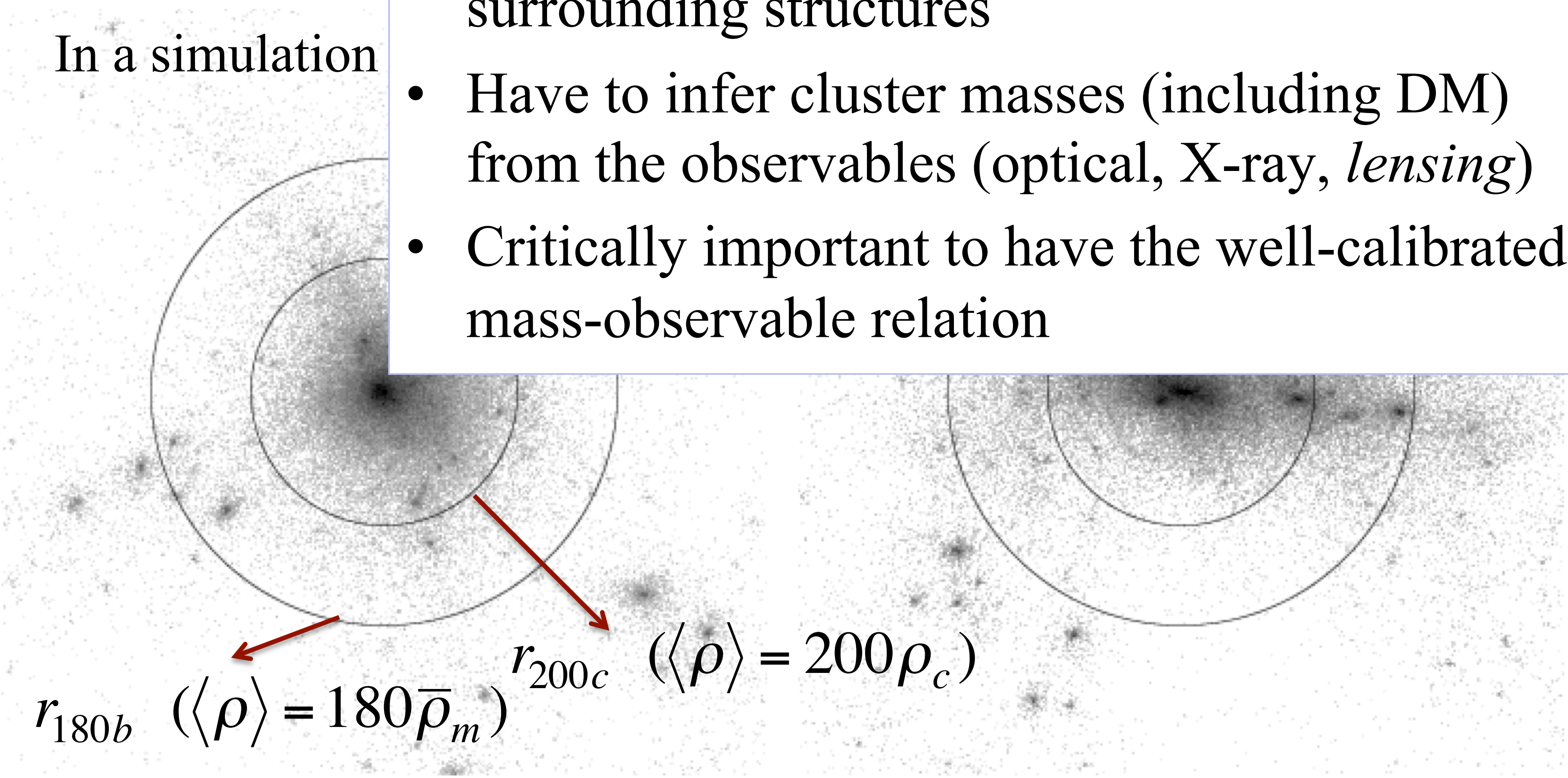

White 02

$$M_\Delta(<r_\Delta) = \int_{r<r_\Delta} d^3\boldsymbol{x}\,\rho(\boldsymbol{x}) \;\Rightarrow\; n(M_\Delta)$$

Cosmological Use of Clusters: Halo Mass Function

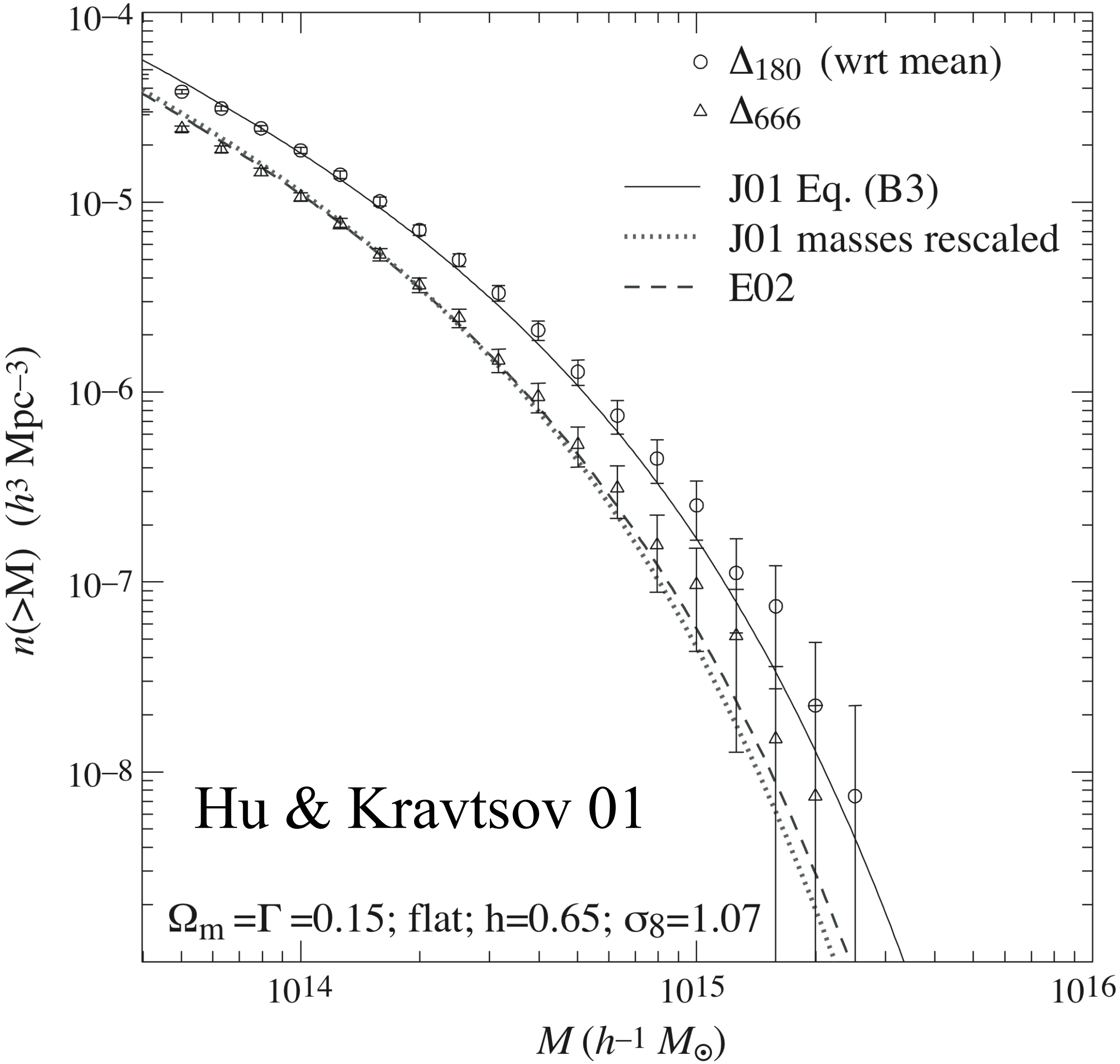

Gaussian seed density fluctuations

+

Spherical collapse model (or N-body simulation)

Mass function: $n(>M)$

$$\frac{dn}{dM} \propto \exp\left(-\frac{\delta_c^2}{2\sigma^2(M)}\right)$$

@cluster mass scales

The mass function can be a powerful probe of cosmology (e.g. DE)

Vikhlinin et al. 0812.2720: Chandra Cluster Cosmology

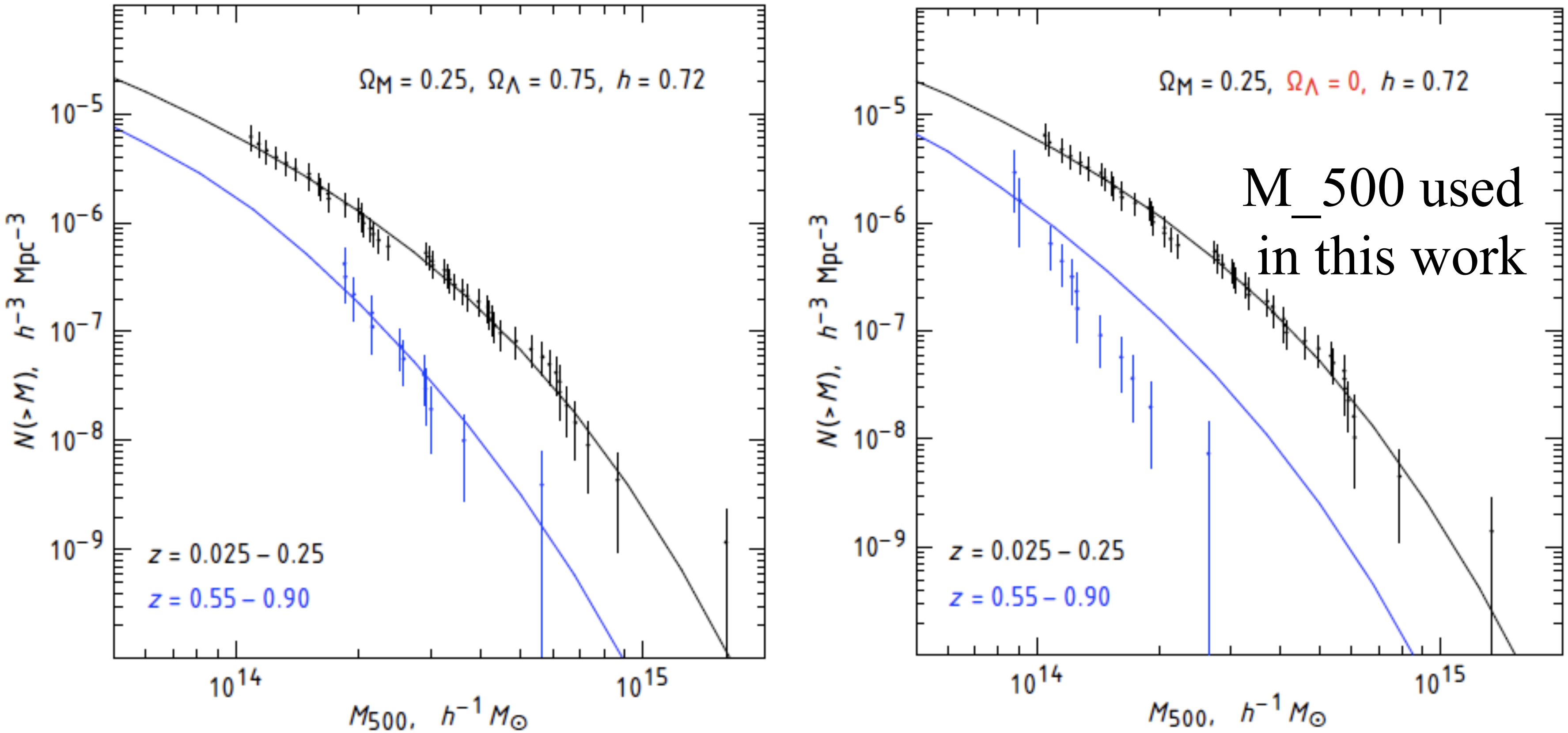

FIG. 2.— Illustration of sensitivity of the cluster mass function to the cosmological model. In the left panel, we show the measured mass function and predicted models (with only the overall normalization at $z = 0$ adjusted) computed for a cosmology which is close to our best-fit model. The low-z mass function is reproduced from Fig. 1, which for the high-z cluster we show only the most distant subsample ($z > 0.55$) to better illustrate the effects. In the right panel, both the data and the models are computed for a cosmology with $\Omega_\Lambda = 0$. Both the model and the data at high redshifts are changed relative to the $\Omega_\Lambda = 0.75$ case. The measured mass function is changed because it is derived for a different distance-redshift relation. The model is changed because the predicted growth of structure and overdensity thresholds corresponding to $\Delta_{crit} = 500$ are different. When the overall model normalization is adjusted to the low-z mass function, the predicted number density of $z > 0.55$ clusters is in strong disagreement with the data, and therefore this combination of Ω_M and Ω_Λ can be rejected.

NFW profile

- An NFW profile is specified by 2 parameters
- Useful to express the NFW profile in terms of the cluster mass and the halo concentration parameter

$$\rho_{\mathrm{NFW}}(r) = \frac{\rho_s}{(r/r_s)(1+r/r_s)^2}$$

$$+\begin{cases} M_\Delta = \dfrac{4\pi}{3} r_\Delta^3 \bar{\rho}_m \Delta & : \text{defines the halo boundary for a given } \Delta \\ M_\Delta = \displaystyle\int_{r<r_\Delta} 4\pi r^2 dr\, \rho_{NFW}(r) & : \text{sets the interior mass of } \rho_{\mathrm{NFW}} \text{ to } M_\Delta \end{cases}$$

$$\Rightarrow \boxed{\rho_{\mathrm{NFW}}(r; M_\Delta, c_\Delta) \quad (\text{note} : c_\Delta \equiv r_\Delta / r_s)}$$

- Can infer the halo mass from the measured halo profile

NFW profile (contd.)

- Dependences of $\rho_{\rm NFW}(r)$ on M and c

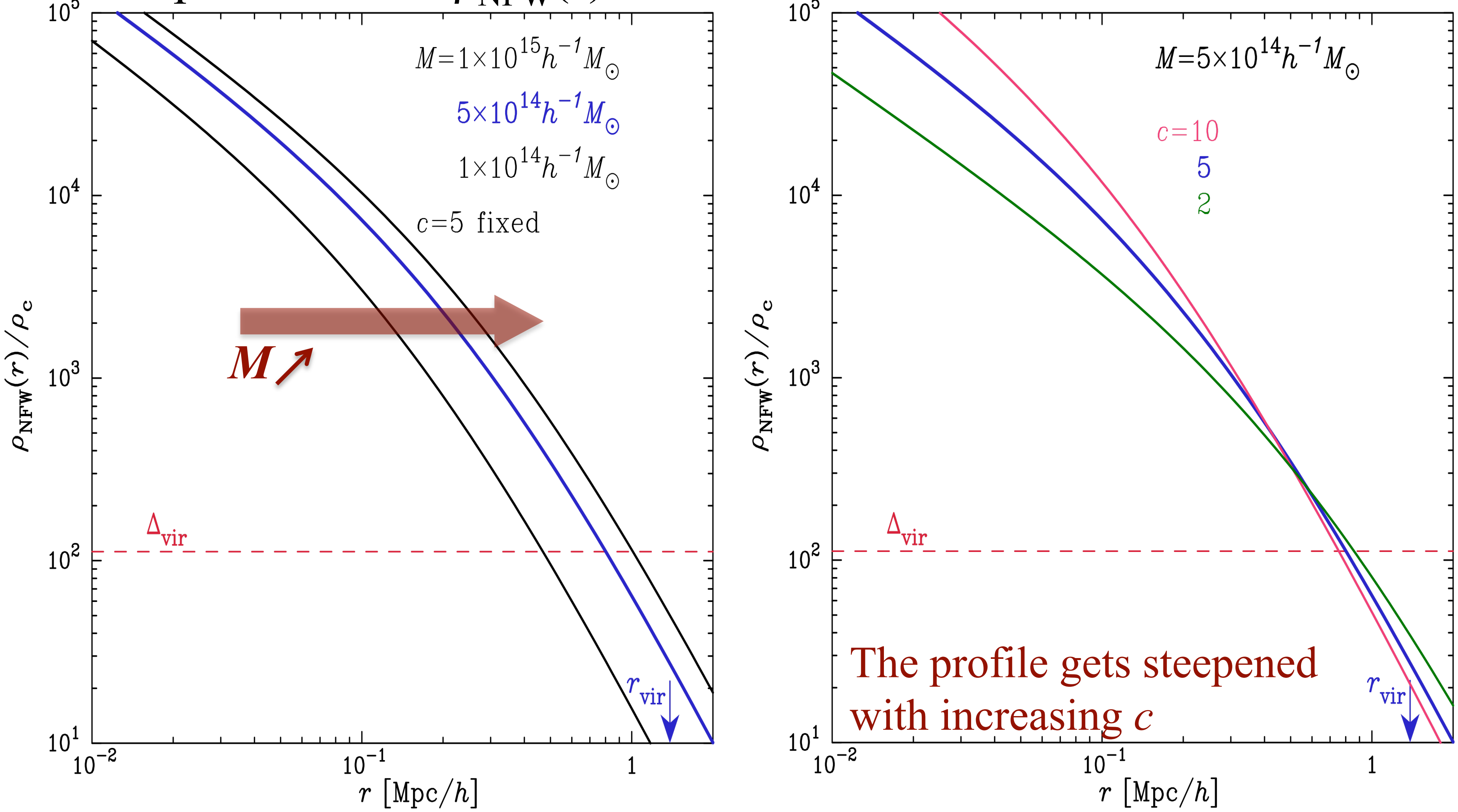

LoCuSS
(The Local Cluster Substructure Survey)

- International collaboration (PI: G.P.Smith; Europe, Japan, USA)
- Explore a systematic study of ~100 X-ray luminous clusters in the redshift range 0.15-0.3
- The multi-wavelengths: Subaru, Palomar, VLT, UKIRT, HST, GALEX, Spitzer, Chandra, XMM, SZA

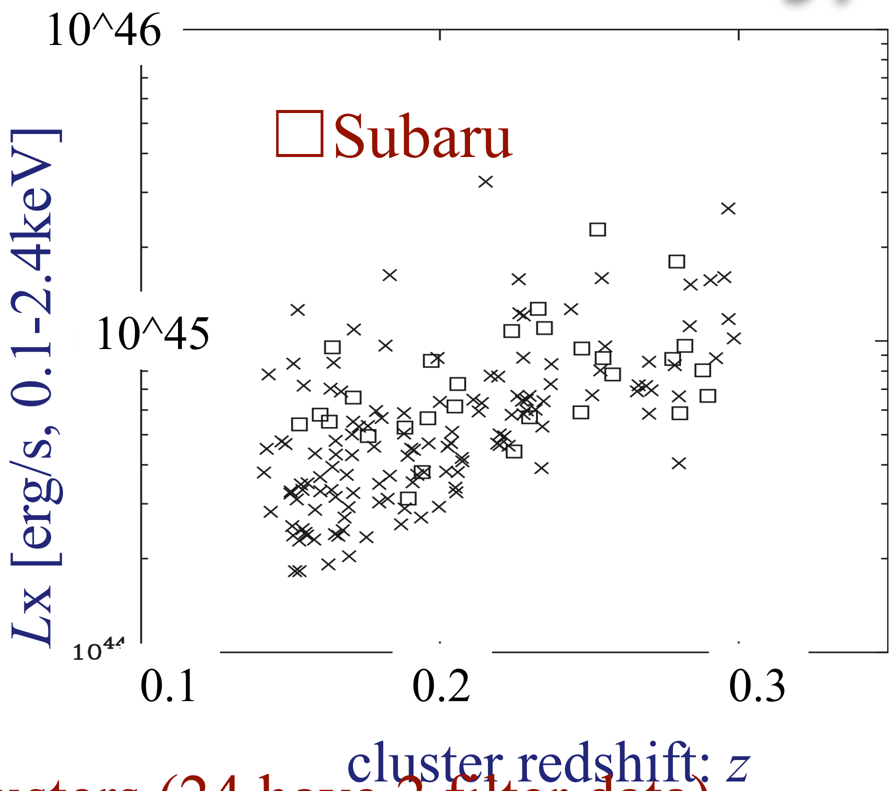

- Subaru/Suprime-Cam data for ~30 clusters (24 have 2 filter data)
  - ***Unbiased*** cluster sample (not based on strong lensing)
  - The FoV of S-Cam matches the virial region of clusters at the target redshifts (~0.2)
  - Add more clusters: ~50 clusters within this year

30 cluster sample (26 clusters with one color)

Name	RA (J2000)	Dec (J2000)	Redshift z	L_X (10^{44}ergs^{-1})	i' (min)	V (min)	seeing (arcsec)
(1)	(2)	(3)	(4)	(5)	(6)	(7)	(8)
A68	00 37 05.28	+09 09 10.8	0.2546	8.81	16.0[a]	30.0[a]	0.83
A115	00 55 59.76	+26 22 40.8	0.1971	8.63	25.0[a]	9.0[d]	0.71
ZwCl0104.4+0048	01 06 48.48	+01 02 42.0	0.2545	5.80	35.0[a]	-	0.65
A209	01 31 53.00	−13 36 34.0	0.2060	7.27	22.0[d]	30.0[d]	0.63
RXJ0142.0+2131	01 42 02.64	+21 31 19.2	0.2803	5.86	40.0[a]	30.0[a]	0.67
A267	01 52 48.72	+01 01 08.4	0.2300	8.11	40.0[a]	30.0[a]	0.61
A291	02 01 44.20	−02 12 03.0	0.1960	5.65	36.0[a]	30.0[a]	0.71
A383	02 48 02.00	−03 32 15.0	0.1883	5.27	36.0[a]	30.0[a]	0.67
A521	04 54 6.88	−10 13 24.6	0.2475	9.46	22.0[d,g]	22.0[d]	0.61
A586	07 32 22.32	+31 38 02.4	0.1710	6.58	35.0[c]	20.0[b]	0.83
ZwCl0740.4+1740[1]	07 43 23.16	+17 33 40.0	0.1114	-	25.0[c]	20.0[c]	0.83
ZwCl0823.2+0425	08 25 57.84	+04 14 47.5	0.2248	4.41	35.0[c]	16.0[c]	0.71
ZwCl0839.9+2937	08 42 56.07	+29 27 25.7	0.1940	3.79	35.0[c]	-	0.77
A611	08 00 55.92	+36 03 39.6	0.2880	8.05	30.0[c]	16.0[c]	0.79
A689	08 37 25.44	+14 58 58.8	0.2793	17.99	40.0[c]	20.0[c]	0.69
A697	08 42 57.84	+36 21 54.0	0.2820	9.64	40.0[c]	16.0[c]	0.73
A750	09 09 11.76	+10 59 20.4	0.1630	5.50	28.0[d]	32.0[d]	0.71
A963	10 17 01.20	+39 01 44.4	0.2060	6.16	I_c, 50.0[d,f]	-	0.75
A1835	14 01 02.40	+02 52 55.2	0.2528	22.80	20.0[b]	20.0[b]	0.89
ZwCl1454.8+2233	14 57 14.40	+22 20 38.4	0.2578	7.80	36.0[b]	15.0[b]	0.81
A2009	15 00 20.40	+21 21 43.2	0.1530	5.40	R_c, 26.0[d,e,g]	-	0.75
ZwCl1459.4+4240	15 01 23.13	+42 20 39.6	0.2897	6.66	R_c, 27.0[d]	18.0[d]	0.57
A2219	16 40 22.56	+46 42 21.6	0.2281	12.07	R_c, 24.0[d]	18.0[d]	0.99
RXJ1720.1+2638	17 20 08.88	+26 38 06.0	0.1640	9.54	32.0[b]	20.0[b]	0.71
A2261	17 22 27.60	+32 07 37.2	0.2240	10.76	R_c, 27.0[d]	18.0[d]	0.63
A2345	21 27 11.00	−12 09 33.0	0.1760	4.95	30.0[a]	-	0.77
RXJ2129.6+0005	21 29 37.92	+00 05 38.4	0.2350	11.00	44.0[a]	30.0[a]	0.85
A2390	21 53 36.72	+17 41 31.2	0.2329	12.69	R_c, 38.0[d]	12.0[d]	0.65
A2485	22 48 31.13	−16 06 25.6	0.2472	5.90	40.0[a]	30.0[a]	0.67
A2631	23 37 40.08	+00 16 33.6	0.2780	7.85	R_c, 24.0[d]	12.0[d]	0.65

“Weak” Gravitational Distortion

Intrinsic shape of a background galaxy (ε~0.3)

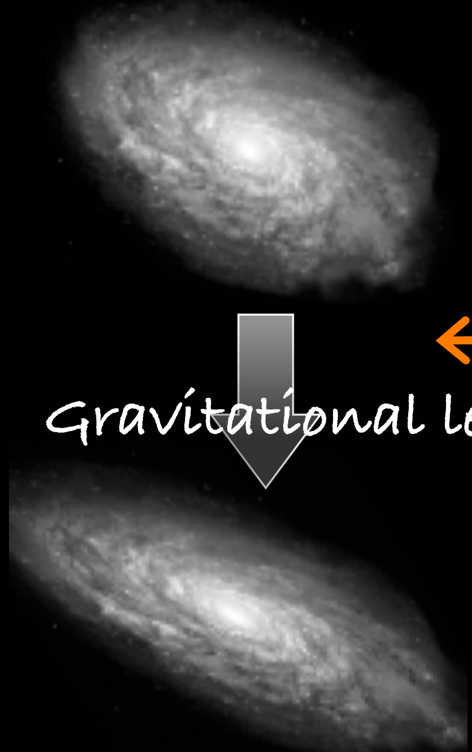

Galaxy shape actually seen after GL: $\varepsilon^{obs} \sim \varepsilon + \gamma^{GL}$

Simulated lensing map

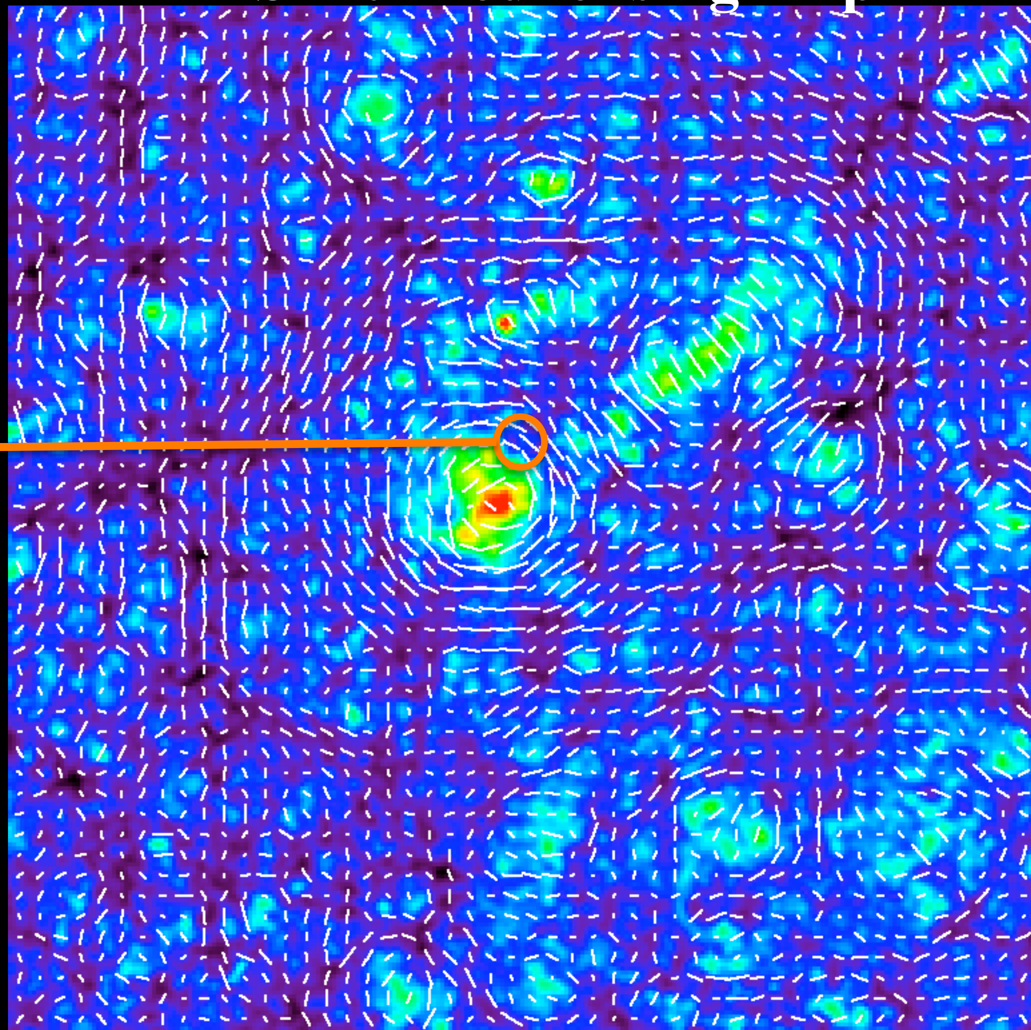

✓The distortion signal of interest is tiny: $\gamma^{GL} \sim 0.01\text{–}0.1$

✓Indeed this coherent signal is statistically measurable

Subaru Telescope: Best facility for WL measurement

- Only Subaru has the prime focus camera, Suprime-Cam, among other 8-10m class telescope: the wide field-of-view (0.25 sq deg)
- Excellent image quality allows accurate shape measurements of galaxies
- Deep images allow the use of many galaxies for the WL: higher spatial resolution

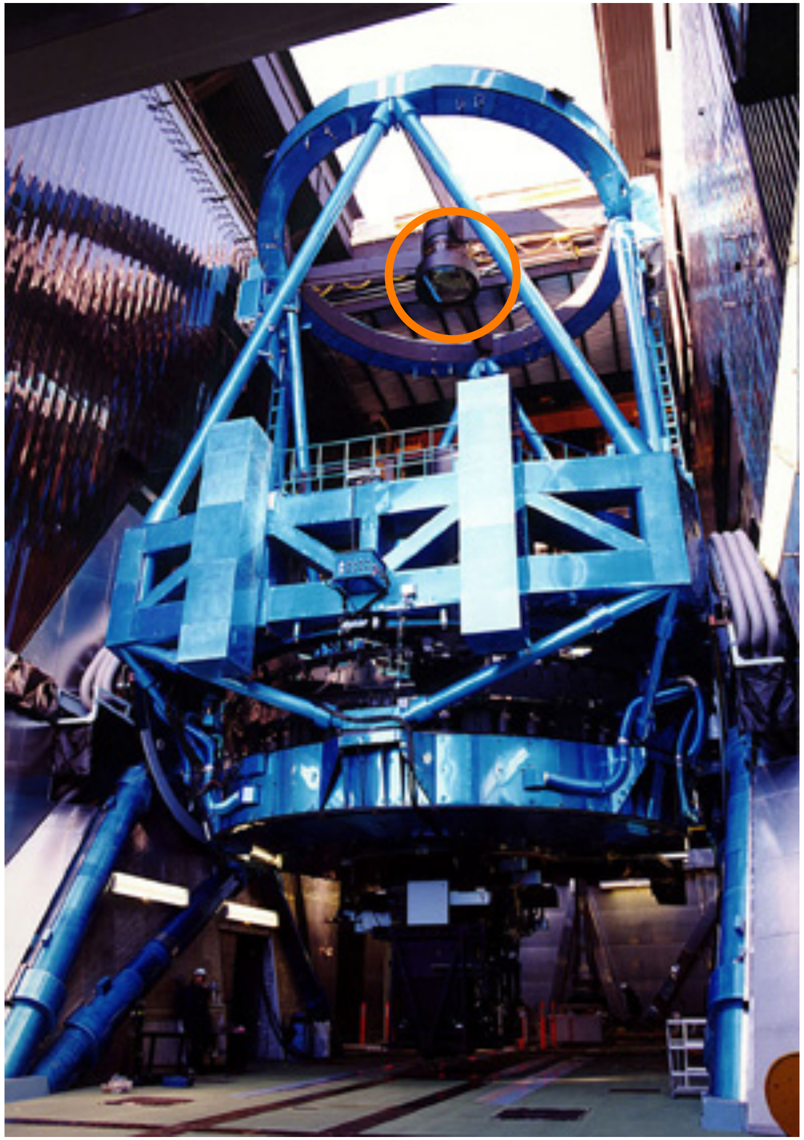

z~0.2 Cluster Shear

- Field of View: 34’ × 27’

E

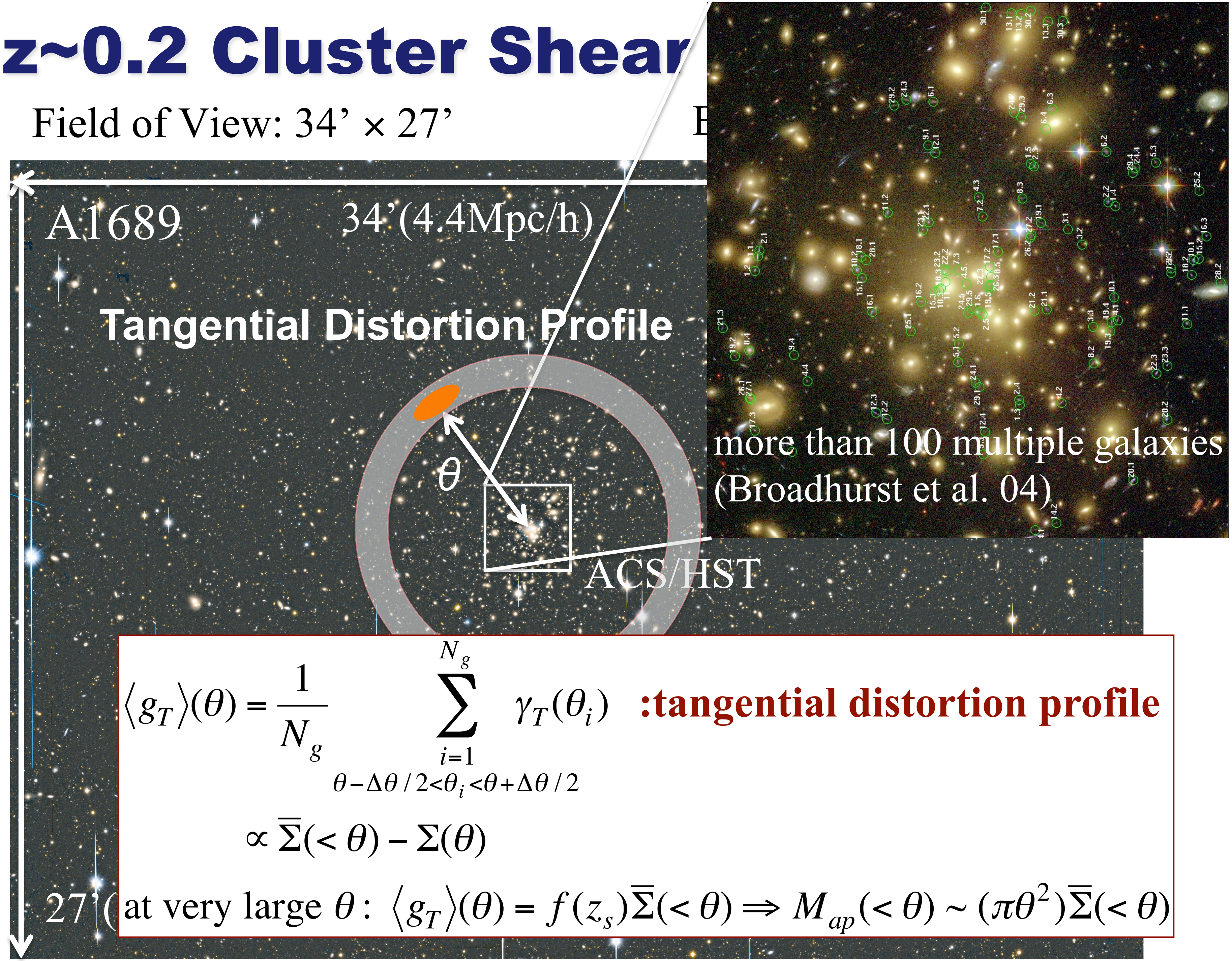

$$\langle g_T \rangle(\theta) = \frac{1}{N_g} \sum_{\substack{i=1 \\ \theta - \Delta\theta/2 < \theta_i < \theta + \Delta\theta/2}}^{N_g} \gamma_T(\theta_i)$$ **:tangential distortion profile**

$$\propto \overline{\Sigma}(<\theta) - \Sigma(\theta)$$

at very large θ: $\langle g_T \rangle(\theta) = f(z_s)\overline{\Sigma}(<\theta) \Rightarrow M_{ap}(<\theta) \sim (\pi\theta^2)\overline{\Sigma}(<\theta)$

Mass Maps

$$\text{shear}: \ \gamma_\alpha \ \Rightarrow \ \text{2D mass density}: \kappa$$

(the different pixels are correlated)

A209

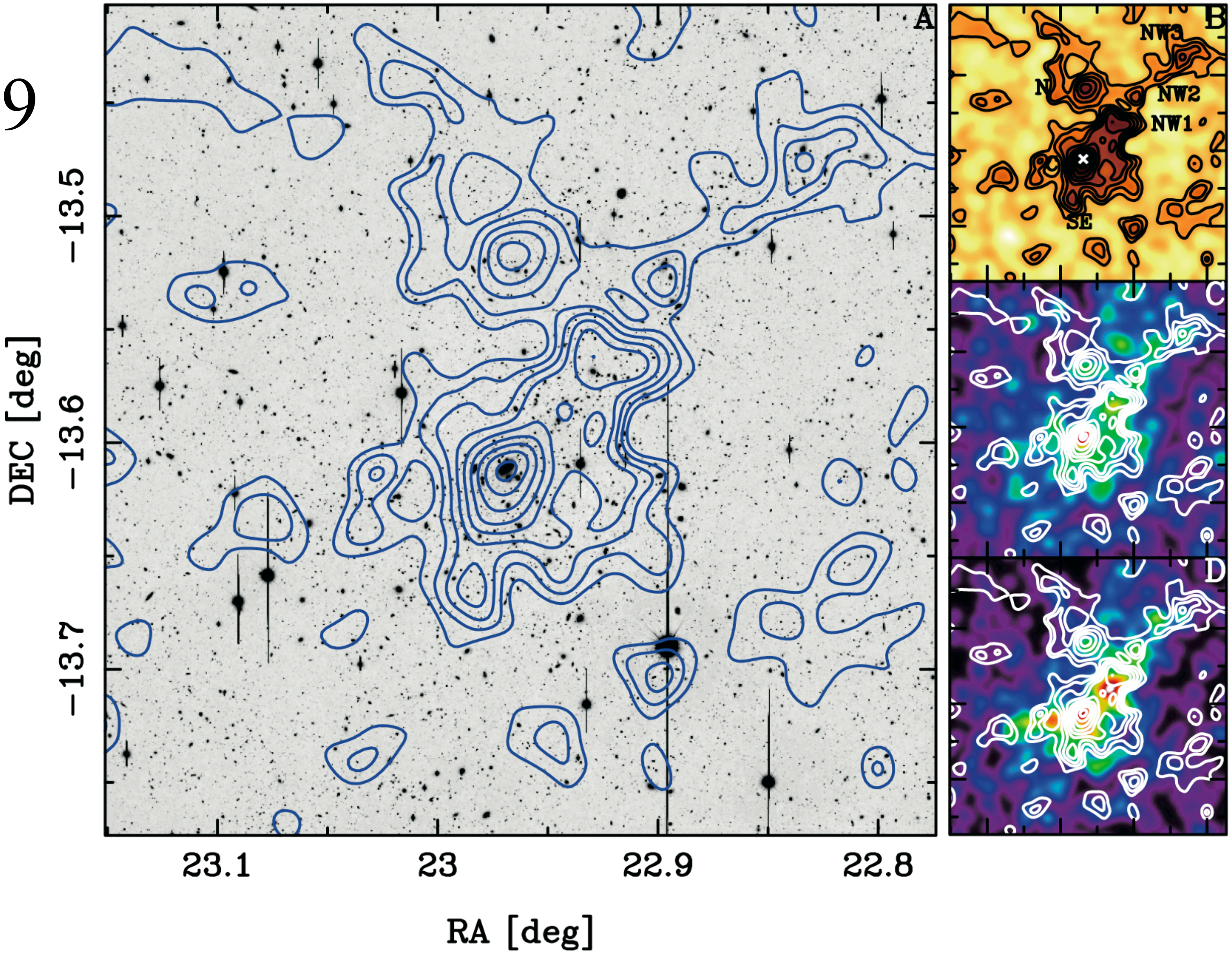

Results: model-dependent constraints

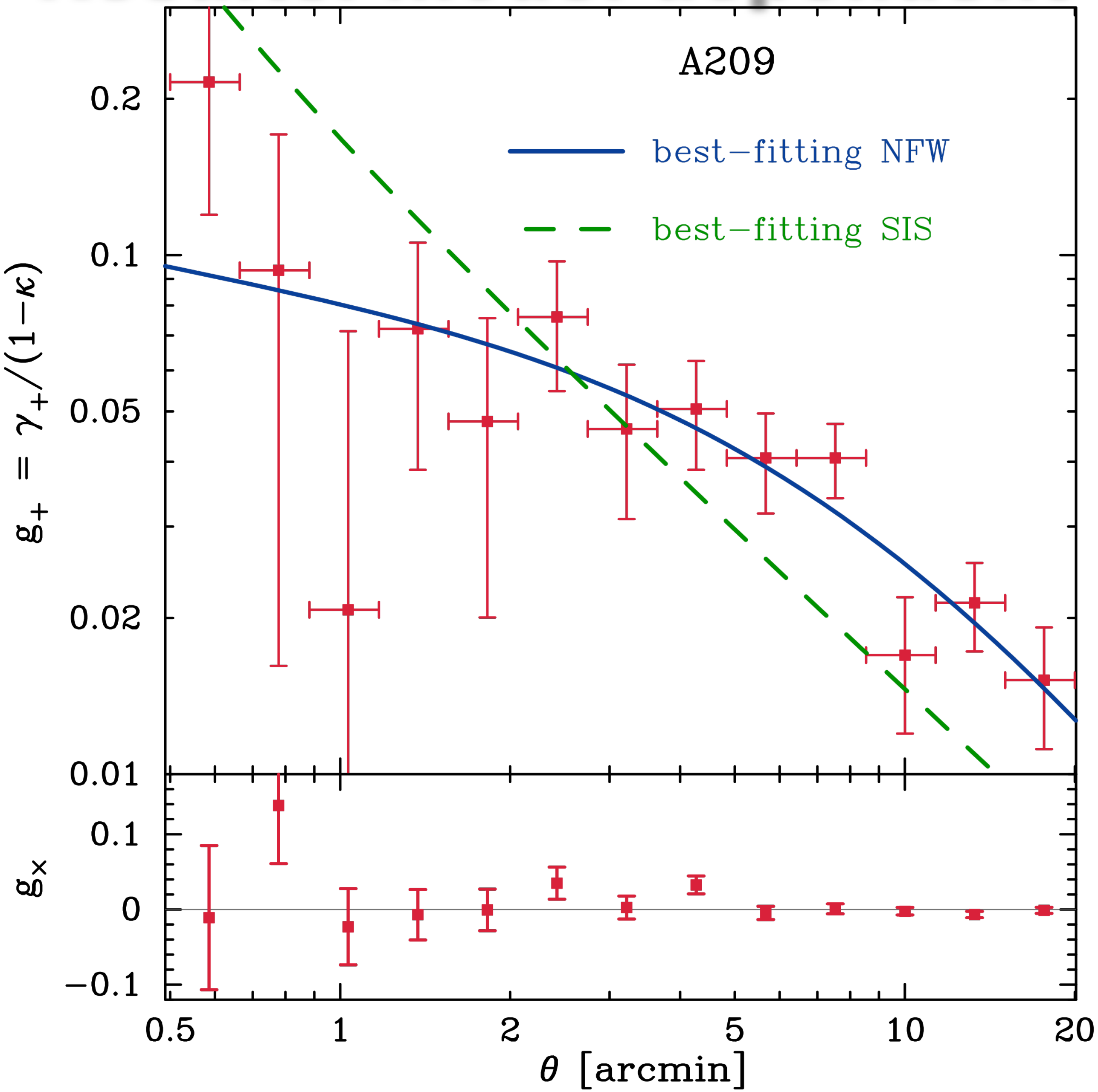

$$\rho_{\mathrm{NFW}} \propto \frac{1}{(r/r_s)(1+r/r_s)^2}$$

$$\rho_{\mathrm{SIS}} \propto \frac{1}{r^2}$$

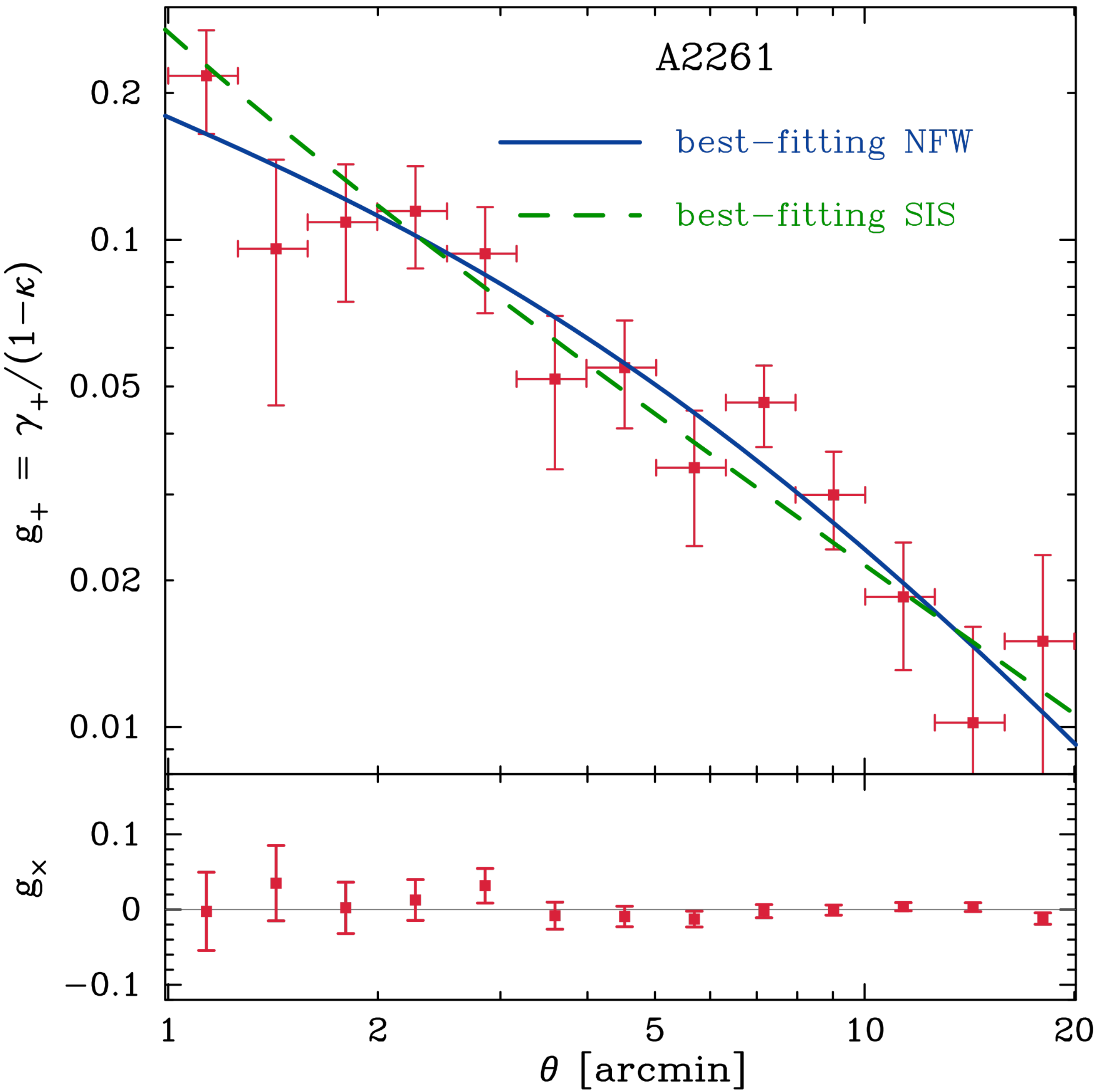

A2261
best−fitting NFW
best−fitting SIS
$g_+ = \gamma_+/(1-\kappa)$
0.2
0.1
0.05
0.02
0.01
$g_\times$
0.1
0
−0.1
1
2
5
10
20
θ [arcmin]

Virial mass estimation

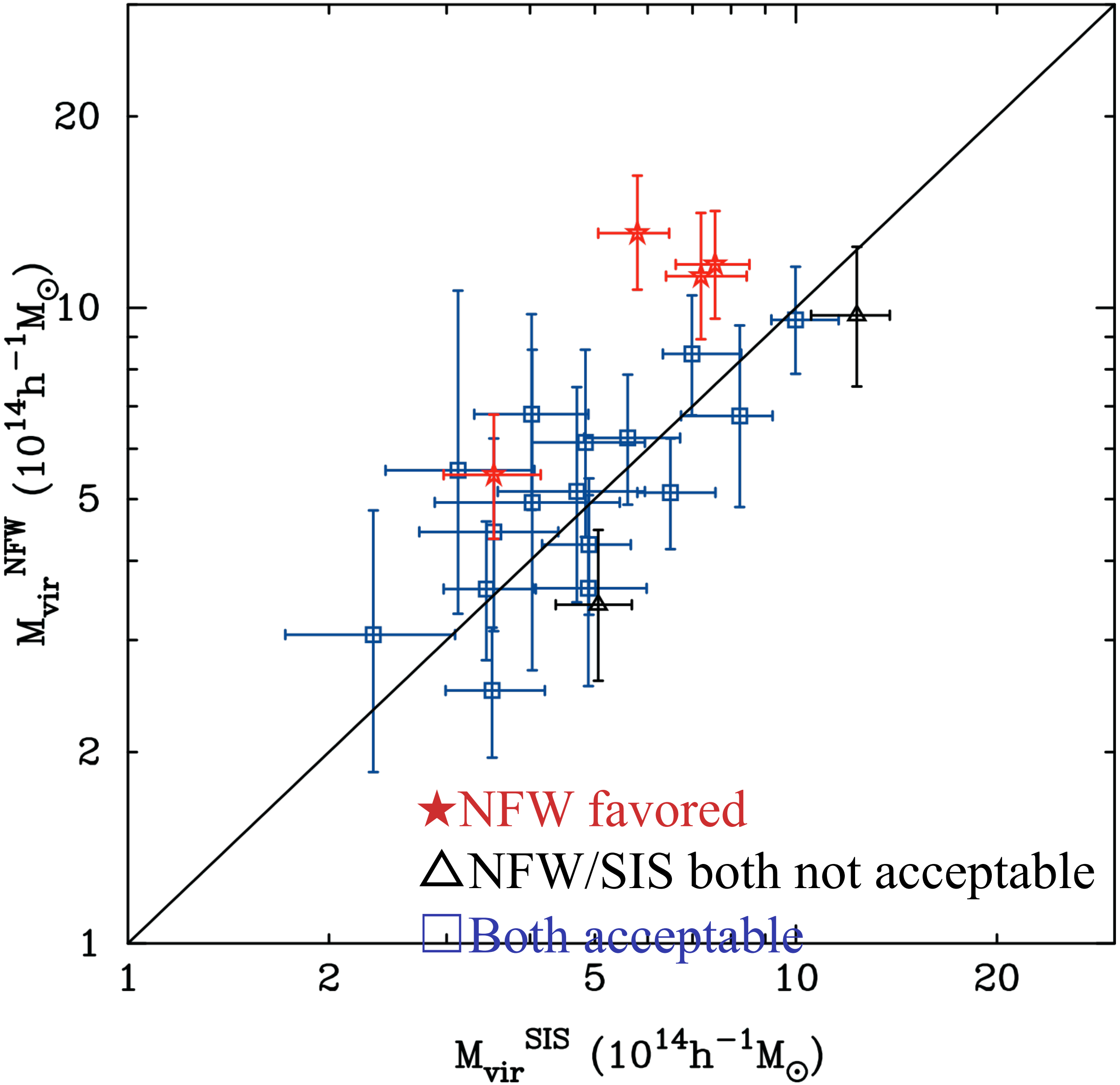

$$\rho_{\mathrm{NFW}} \propto \frac{1}{(r/r_s)(1+r/r_s)^2}$$

$$\rho_{\mathrm{SIS}} \propto \frac{1}{r^2}$$

- The mass estimates depend on the model assumed for the fitting
- The virial mass determination: accuracy 20-30%
- $M_{NFW}/M_{SIS} \sim 1.19$

Mass determination (contd.)

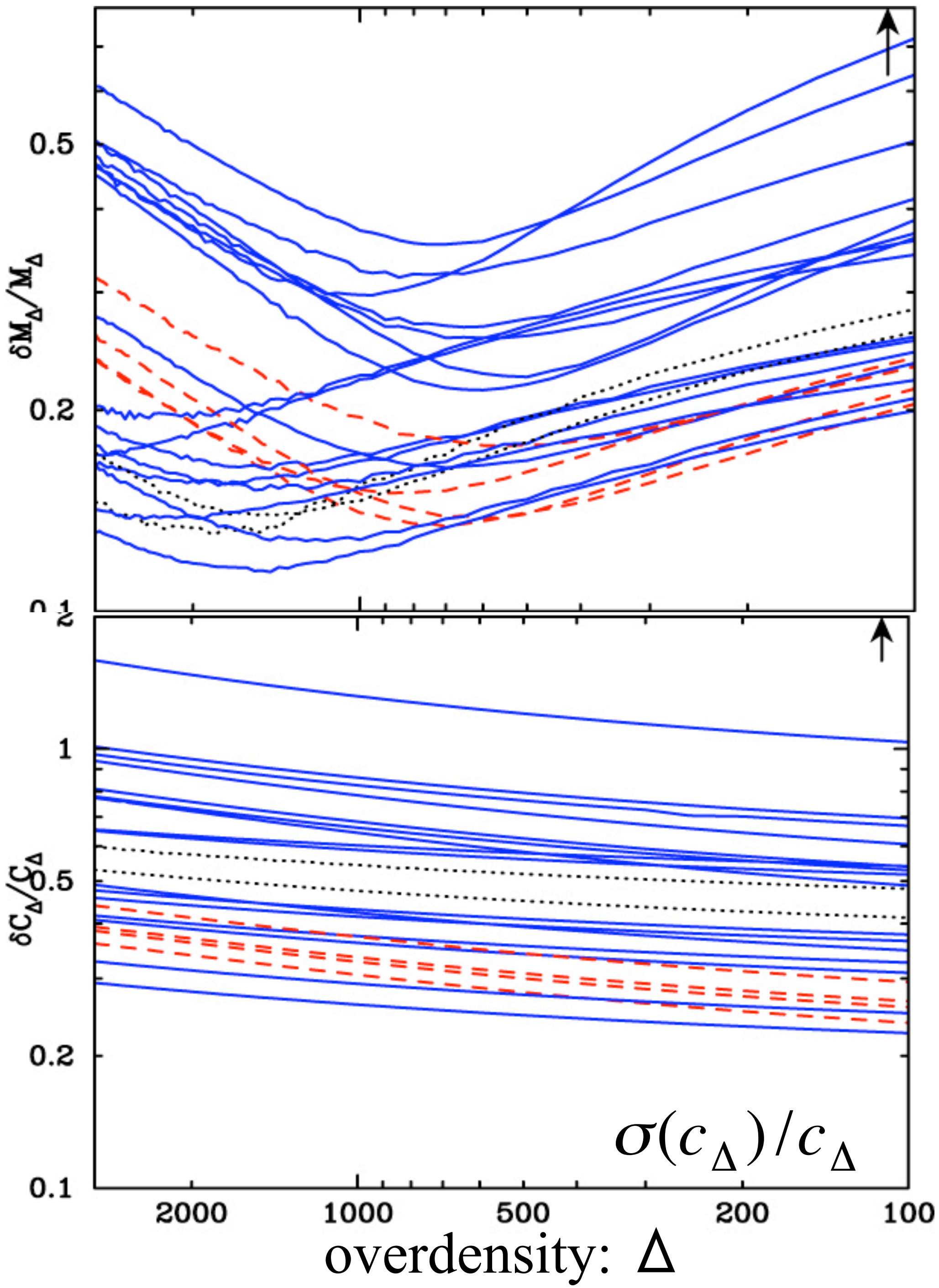

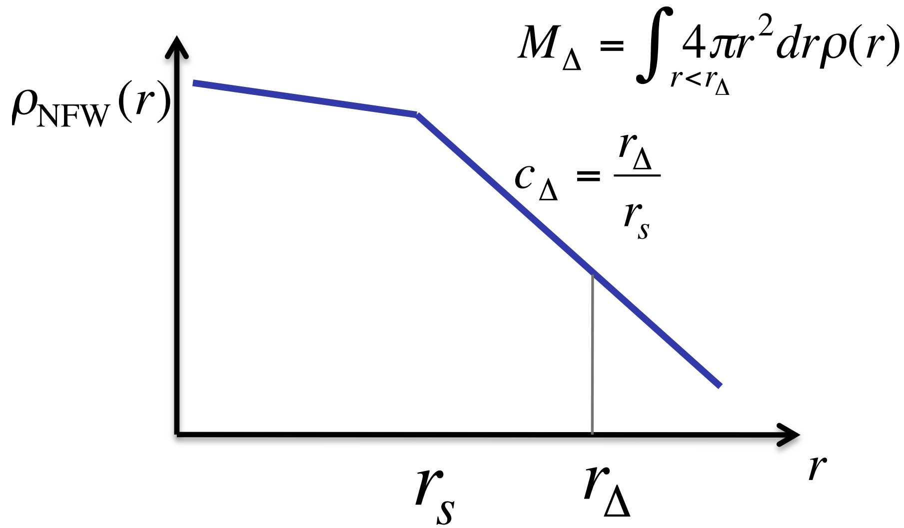

- A best accuracy in M is 10-20% when Δ=500-1000 is assumed
  - Over the radii the lensing signals have a largest S/N
- The concentration parameter is most accurately measured for the virial definition

Stacked Lens

- Advantage: effects due to halo asphericity, substructure, unassociated structures along the same l.o.s. are averaged out by the stacking average

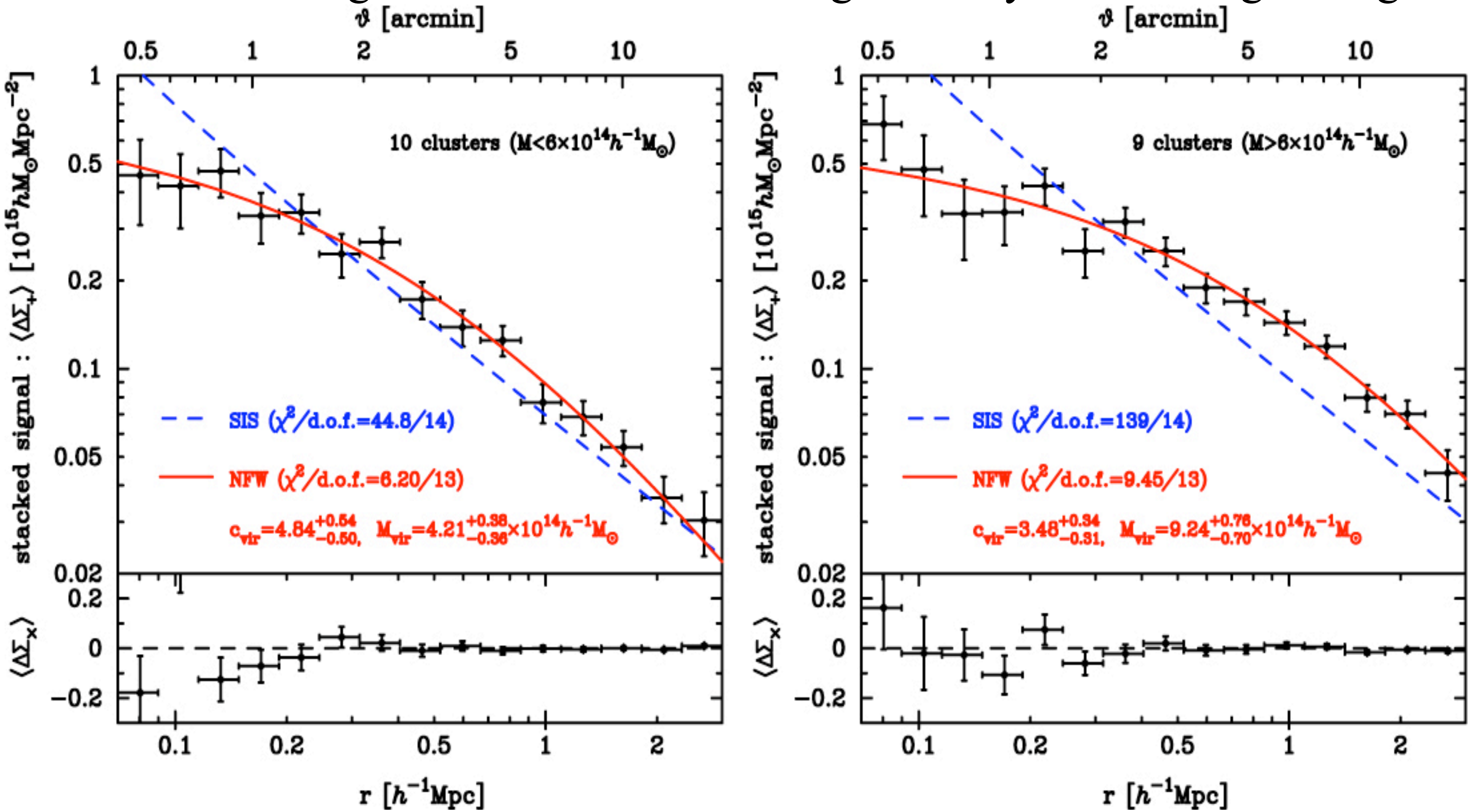

$$\Delta\chi^2 = \chi^2_{\mathrm{SIS}} - \chi^2_{\mathrm{NFW}} = 39 \text{ and } 129 \text{ for low- and high-mass samples, respectively}$$

The observed *C*(*M*) relation

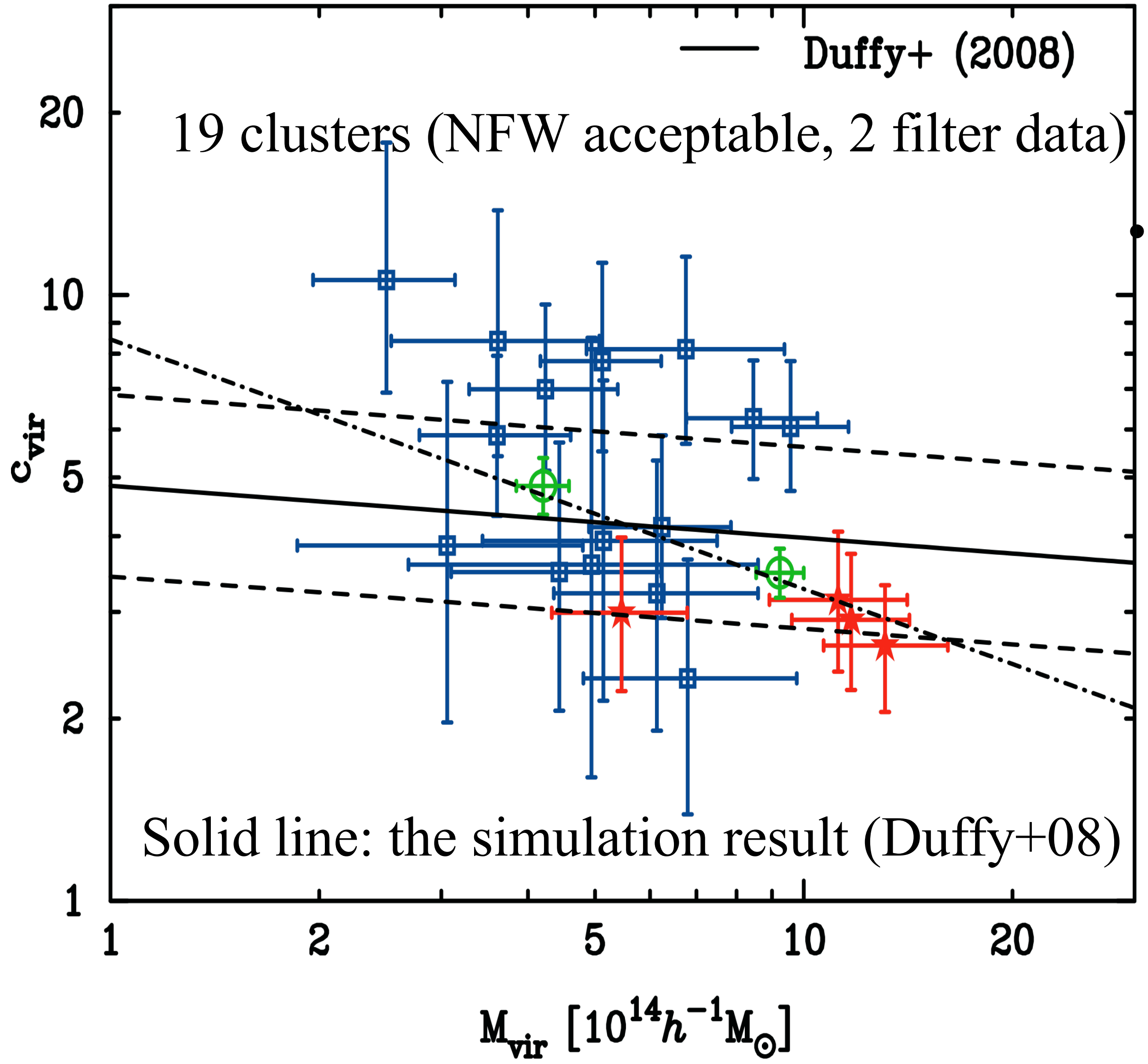

The first-time results of *C*(*M*) based on WL

- Fitting to the relation

$$c(M) = c_N \left(\frac{M_{vir}}{10^{14} h^{-1} M_{sun}} \right)^{-\beta}$$

$$c_N = 8.45^{+3.91}_{-2.80} \Leftrightarrow c_{exp} \sim 5$$
$$\beta = 0.41 \pm 0.19 \Leftrightarrow \beta_{exp} \sim 0.1$$

A 2σ-level detection of the C-M relation, but a much steeper relation than theoretically expected

1D distribution of *C*

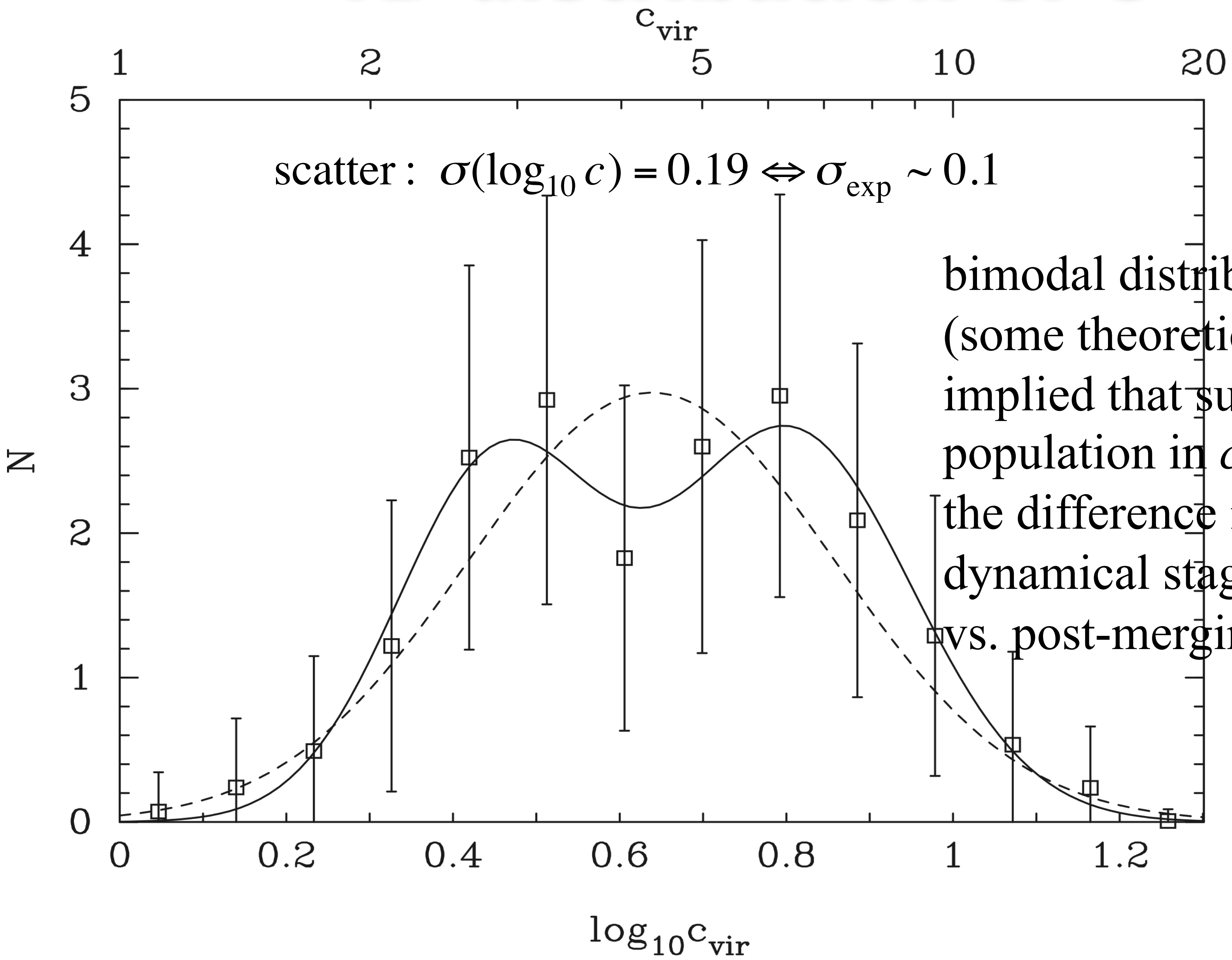

$$\text{scatter}: \ \sigma(\log_{10} c) = 0.19 \Leftrightarrow \sigma_{\exp} \sim 0.1$$

bimodal distribution?
(some theoretical studies implied that such two population in *c* arise from the difference in the dynamical stages, relaxed vs. post-merging phase)

Aperture mass method
- model-independent estimate of 2D mass -

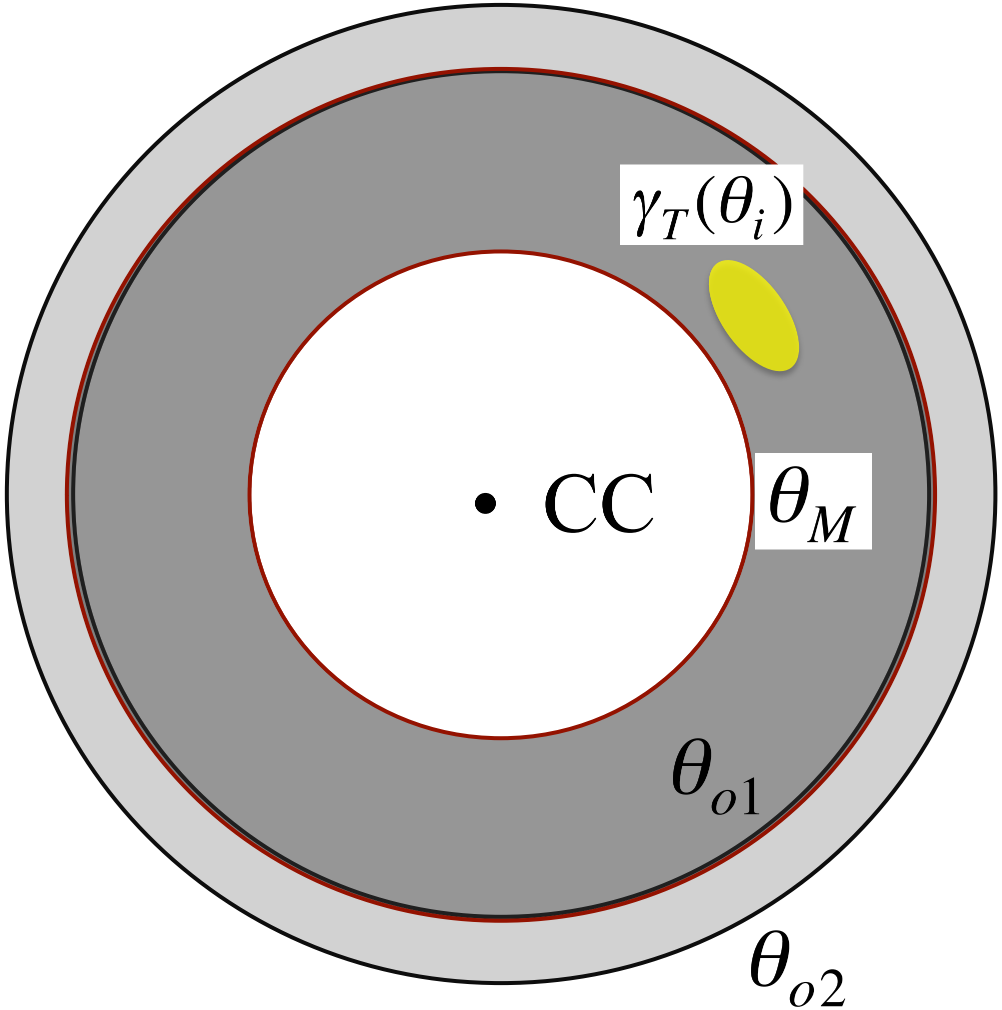

Use the measured shear profile at radii greater than θ_M (don't use the inner-radius shear)

$$\zeta(\theta_M) = 2\int_{\theta_M}^{\theta_{o1}} d\ln\theta \langle\gamma_T\rangle(\theta) - \frac{2}{1-\theta_{o1}^2/\theta_{o2}^2}\int_{\theta_{o1}}^{\theta_{o2}} d\ln\theta\langle\gamma_T\rangle(\theta)$$

$$\propto \frac{M_{2D}(<\theta_M)}{\pi\theta_M^2} - \frac{M_{2D}(\theta_{o1}<\theta<\theta_{o2})}{\pi(\theta_{o2}^2-\theta_{o1}^2)}$$

if $M_{2D}(\theta_{o1}<\theta<\theta_{o2}) \approx 0$

$$\boxed{M_{2D}(<\theta_M) \approx \pi\theta_M^2\zeta(\theta_M)\Sigma_{\rm cr}}$$

Model-independent mass estimate: 2D Mass vs. 3D Mass

2D Mass = Projected mass along the l.o.s.

$M_{2D}(<r_\Delta) \sim \pi r_\Delta^2 \langle g_T \rangle (\theta_\Delta)$

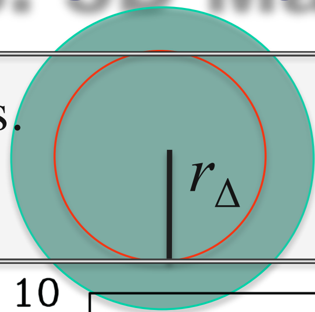

3D mass: $M_{\rm NFW}(<r_\Delta)$

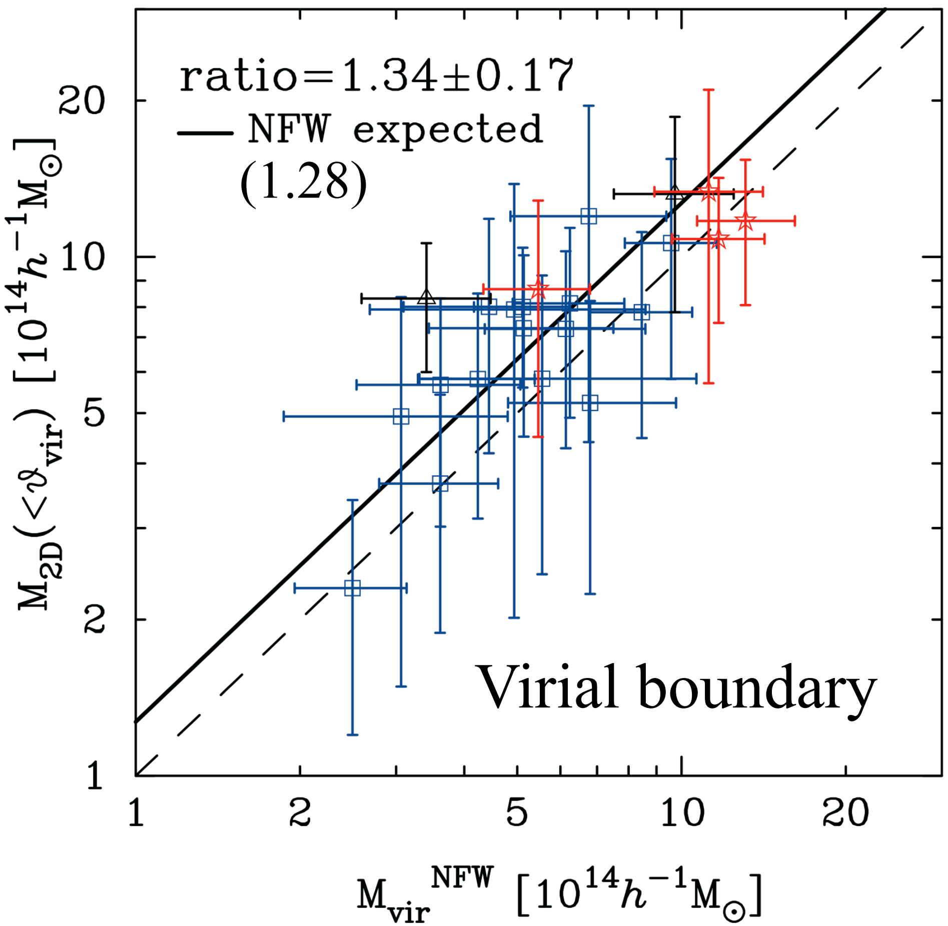

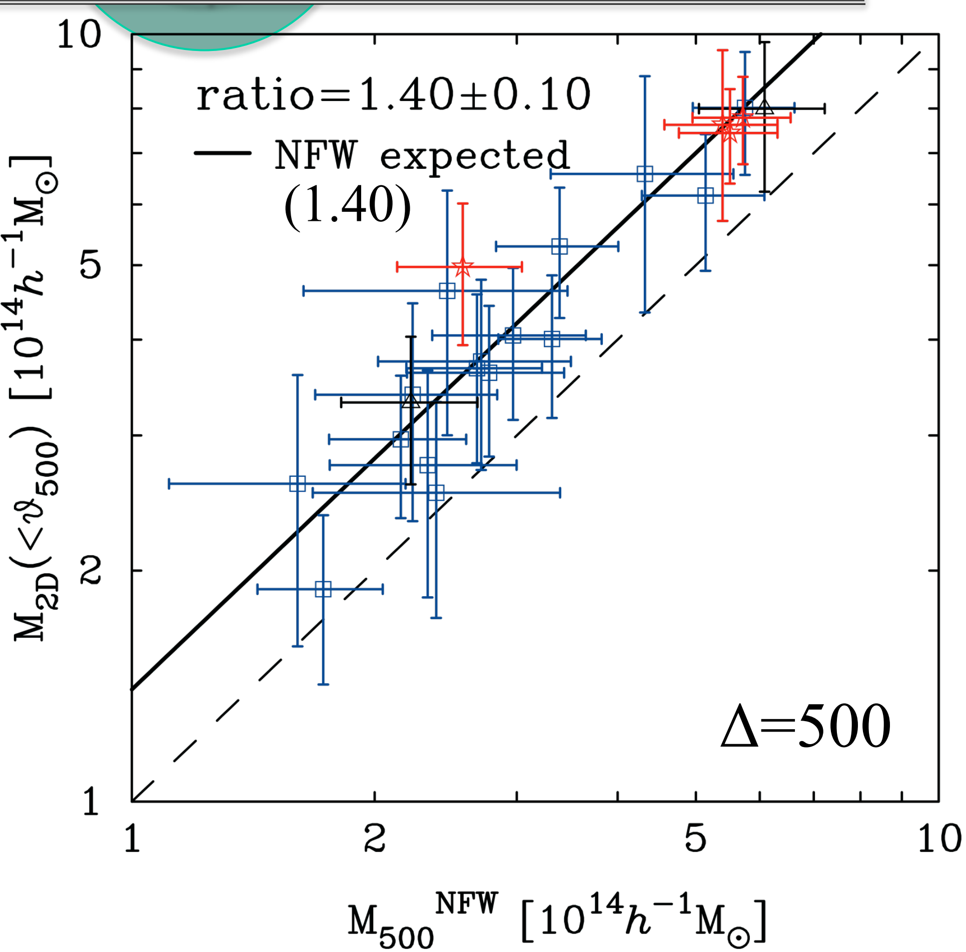

Dilution contamination

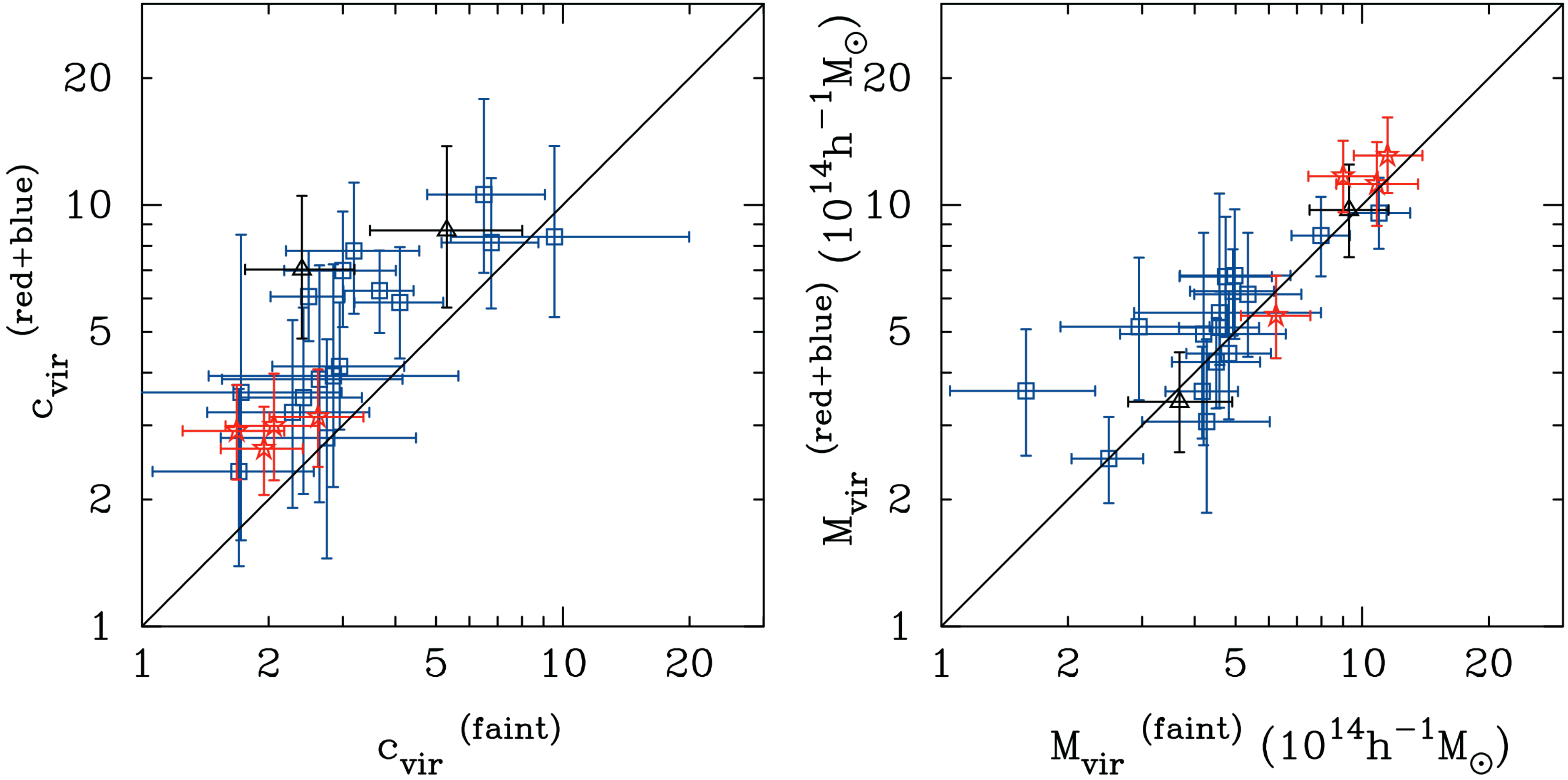

- The faint galaxy sample is very likely to be contaminated by unlensed, member galaxies
- The dilution effect causes the concentration to be significantly underestimated, but doesn't change the virial mass estimation

Summary

- The ability assessment of a ground-based WL method for estimating cluster masses (Subaru)
  - Model fitting method:
    - Important to assume an appropriate mass model (NFW)
    - 10-20% accuracy in $\delta M/M$ for $\Delta \sim 500$-1000
    - Stacked lensing vs. individual lensing: important to understand scatters and bias in mass-observable relation
    - 2D model fitting: working in progress
  - Model independent method:
    - Use the shear signals at outer radii (not sensitive to the inner mass distribution, i.e. concentration)
    - Probe 2D mass, but correctable
- Towards obtaining a well-calibrated mass proxy relation
  - LoCuSS sample (Subaru, X-ray, SZA, dynamical): a well-calibrated low-z sample (just like low-z SNe)

welcome program participants registration venue organizers contact

IPMU international conference

dark energy: lighting up the darkness!

Institute for the Physics and Mathematics of the Universe
the University of Tokyo
Kashiwa, Japan
June 22 - 26, 2009

"One cannot avoid the darkness unless one knows where it lies and the routes that lead to it"
master Tolaris Shim, Star Wars

Invited speakers

Hiroaki Aihara (IPMU)
Luca Amendola (Roma)
Gary Bernstein (Penn)
John Carlstrom (Chicago)
Joanna Dunkley (Oxford)
Daniel Eisenstein (Arizona)
Shirley Ho (LBL)
Tsuneyoshi Kamae (SLAC)
Daniel Kasen* (Santa Cruz)
Ofer Lahav (UCL)
Yannick Mellier* (IAP)
Joseph J. Mohr (Illinois)
Shinji Mukohyama (IPMU)
Masamune Oguri (KIPAC)
Saul Perlmutter* (LBL)
Mohammad Sami (Jamia Millia Islamia)
Uros Seljak (Berkeley)
Suzanne T. Staggs (Princeton)
Paul J. Steinhardt (Princeton)
David N. Spergel (Princeton/IPMU)
Michael S. Turner (Chicago)
Alexey Vikhlinin (CfA)
Naoki Yasuda (IPMU)

IPMU INSTITUTE FOR THE PHYSICS AND MATHEMATICS OF THE UNIVERSE
wpi World Premier International Research Center Initiative
東京大学 THE UNIVERSITY OF TOKYO